African horse sickness virus induces apoptosis in cultured mammalian cells

Liesel Stassen[a] Henk Huismans[b] Jacques Theron[a]

[a]Department of Microbiology and Plant Pathology, University of Pretoria, Pretoria 0002, South Africa

[b]Department of Genetics, University of Pretoria, Pretoria 0002, South Africa

*Corresponding Author: Prof J. Theron
Department of Microbiology and Plant Pathology
University of Pretoria
Pretoria 0002
South Africa

E-mail: jacques.theron@up.ac.za
Tel: +27 12 420-2994
Fax: +27 12 420-3266

Abstract

Infection of mammalian cell cultures with African horse sickness virus (AHSV) is known to result in dramatic cytopathic effects (CPE), but no CPE is observed in infected insect cell cultures despite productive virus replication. The basis for this phenomenon has not yet been investigated, but is suggestive of apoptosis being induced following virus infection of the mammalian cells. To investigate whether AHSV can induce apoptosis in infected mammalian cells, *Culicoides variipennis* (KC) insect cells and BHK-21 mammalian cells were infected with AHSV-9 and analyzed for morphological and biochemical hallmarks of apoptosis. In contrast to KC cells, infection of BHK-21 cells with AHSV-9 resulted in ultrastructural changes and nuclear DNA fragmentation, both of which are associated with the induction of apoptosis. Results also indicated that AHSV-9 infection of BHK-21 cells resulted in activation of caspase-3, a key agent in apoptosis, and in mitochondrial membrane depolarization. Cumulatively, the data indicate that the intrinsic pathway is activated in AHSV-induced apoptosis.

Keywords: African horse sickness virus; Apoptosis; BHK-21 cells; *Culicoides variipennis* cells; Caspases; Intrinsic pathway

African horse sickness virus (AHSV) is a species in the genus *Orbivirus*, family *Reoviridae* (Calisher and Mertens, 1998), and is the causative agent of African horse sickness (AHS), a highly infectious arthropod-borne (*Culicoides* spp.) disease of equids, of which the mortality rate in horses may exceed 90% (Coetzer and Erasmus, 1994; Guthrie, 2007). Although African horse sickness virus (AHSV) causes severe oedema and haemorrhages in horses, it is asymptomatic in the insect host (Mellor and Hamblin, 2004; Wilson et al., 2009). This is also reflected in tissue culture where AHSV causes rapid cell death in infected mammalian cells in culture, whereas infection of insect cells are unapparent and show no CPE (Mirchamsy et al., 1970; Osawa and Hazrati, 1965). The basis for this differential host response is not known, but may be due to the induction of apoptosis in infected mammalian cells. Indeed, analyses of endothelial cells of animals infected with AHSV indicated ultrastructural changes that could be suggestive of apoptosis (Gómez-Villamandos et al., 1999). Apoptosis is a selective process of physiological cell deletion in response to numerous developmental and environmental stimuli (Kerr et al., 1972). There are two common pathways for the induction of apoptosis, *i.e.* the extrinsic pathway, which is primarily initiated by virus attachment to receptors, and the intrinsic pathway, which is mediated by damage to the mitochondria (Duprez et al., 2009). Various reports have indicated that infection of mammalian cells by viruses induces apoptosis (Roulston et al., 1999) and in some virus-induced diseases, apoptosis is a pathogenic mechanism that contributes in vivo to cell death, tissue injury and disease severity (Clarke and Tyler, 2009; Clarke et al., 2009; Samuel et al., 2007). Indeed, the induction of apoptosis has recently been implicated in the pathogenesis of bluetongue virus (BTV), the prototype orbivirus, in sheep (Umeshappa et al., 2010). In the present study, AHSV-infected insect and mammalian cells were analyzed for morphological and biochemical hallmarks of apoptosis. We report that, in contrast to insect cells, apoptosis was

induced in mammalian cells in response to AHSV infection. We furthermore show that AHSV infection induces the intrinsic apoptosis pathway in mammalian cells with the activation of caspase-3.

BHK-21 cells were cultured in Minimum Essential Medium (MEM) (Sigma-Aldrich) containing 5% fetal bovine serum (FBS), 60 mg/ml penicillin, 60 mg/ml streptomycin and 150 µg/ml Fungizone (Highveld Biological). Embryonic *Culicoides variipennis* (KC) cells were maintained in modified Schneider's *Drosophila* medium supplemented with 10% FBS, 60 mg/ml penicillin, 60 mg/ml streptomycin and 150 µg/ml Fungizone (Highveld Biological). BHK-21 and KC cell monolayers were either mock-infected or infected with AHSV-9 (kindly provided by Mr. F. Wege, Department of Genetics, University of Pretoria) at a multiplicity of infection (MOI) of 1 PFU/cell, and analyzed over a time course of 72 h (BHK-21 cells) or 7 days (KC cells) post-infection. Immunoblot analysis of the infected BHK-21 (Fig. 1A) and KC (Fig. 2A) cells, using an anti-AHSV-9 polyvalent serum (Onderstepoort Veterinary Institute) confirmed expression of viral proteins. Apoptotic cells exhibit characteristic morphological features that include cell membrane blebbing, chromatin condensation and the formation of apoptotic bodies (Martelli et al., 2001; Wyllie et al., 1981). Consequently, mock-infected and AHSV-infected BHK-21 and KC cell monolayers were examined for AHSV-induced cytopathic effects (CPE) with a Zeiss Axiovert 200 inverted microscope, and, for the detection of morphological cell alterations characteristic of apoptosis, cells were prepared for examination by a Philips 301 transmission electron microscope. Light microscopy of the AHSV-infected BHK-21 cells at 72 h post-infection indicated severe CPE (Fig. 1B). In contrast to mock-infected BHK-21 cells, virus infection resulted in cell rounding, shrinkage and surface detachment. Subsequent TEM analysis of the virus-infected BHK-21 cells showed condensation of chromatin, nuclear fragmentation into apoptotic bodies and plasma membrane blebbing (Fig. 1C). DNA cleavage and proteolysis of key nuclear polypeptides are responsible for these morphological changes that occur during apoptosis (Fischer et al., 2003). Despite production of viral proteins in AHSV-infected KC cells (Fig. 2A), microscopic examination (Fig. 2B) and transmission electron micrographs (Fig. 2C) did not display any morphological features that could be associated with apoptotic events. Indeed, at 7 days post-infection virus-infected KC cells were indistinguishable from the mock-infected KC cells. These results therefore suggested that, in contrast to AHSV-infected BHK-21 mammalian cells, apoptosis was not induced in virus-infected KC insect cells.

In cells undergoing apoptosis, morphological changes are associated with the incidence of nucleosome excisions from chromatin through the activation of an intracellular endonuclease, thereby resulting in the appearance of a nucleosomal DNA ladder (Wyllie, 1980). Consequently, chromosomal DNA was extracted from mock-infected or AHSV-infected BHK-21 cells (*ca.* 2×10^6 cells) with an Apoptotic DNA-ladder kit (Roche Diagnostics) and analyzed by agarose gel electrophoresis for nuclear DNA fragmentation (Fig. 3A). Lyophilized apoptotic U937 cells served as a positive control of chromosomal DNA fragmentation, whereas AHSV-infected KC cells were included in the analysis to verify the absence of apoptosis (Fig. 3B). In contrast to mock-infected BHK-21 cells, which showed no evidence of DNA fragmentation, an oligonucleosomal DNA ladder was detected in AHSV-infected cells from 12 to 72 h post-infection, and resembled that observed in apoptotic U937 cells (Fig. 3A). Furthermore, fragmentation of the chromosomal DNA in AHSV-infected BHK 21 cells at 72 h post-infection appears to be precise and non-random, as evidenced in a second independent sample that displayed an identical

DNA-laddering pattern. In contrast, there was no detectable chromosomal DNA fragmentation in the AHSV-infected KC cells over a time course of 7 days (Fig. 3B). These results therefore provided biochemical evidence that the gross morphological changes observed in AHSV-infected BHK-21 cells was due to the induction of apoptosis in the mammalian cells. To determine more accurately when apoptosis is induced in the AHSV-infected BHK-21 cells, the nucleosomes present in the cytoplasm of virus-infected cells was quantified over a time course of 72 h using the Cell Death Detection ELISA^{PLUS} kit (Roche Diagnostics). This assay is based on a sandwich-enzyme immunoassay principle using monoclonal antibodies directed against histones and DNA, respectively. The results, presented in Fig. 3C, indicated a limited increase (0.6-fold) of nucleosomes into the cytosol of AHSV-infected BHK-21 cells during the first 6 h of infection, followed by a significant increase (12-fold) between 6 and 12 h post-infection. Between 12 and 24 h post-infection, there was a slight increase (1.4-fold) in the release of nucleosomes, and thereafter no further increases in the nucleosome enrichment factor was observed. The DNA laddering pattern became more random from 48 h post-infection onwards, most likely due to non-specific nucleolysis of already fragmented nuclear DNA (Koyama and Adachi, 1997). These results therefore indicate that apoptosis was induced at 12 h post-infection and maximal apoptosis is reached at 24 h post-infection.

To gain insight into the mechanism of AHSV-induced apoptosis, activation of caspase-3, the effector caspase in both the extrinsic and intrinsic apoptotic pathways (Duprez et al., 2009) was determined with an ApoTarget™ Caspase-3 Colorimetric Protease Assay kit (BioSource International). At the end of the respective incubation periods, mock- and AHSV-infected BHK-21 cells (*ca.* 2.5×10^6 cells) were lysed, and protein concentration in the cytosol extract was determined with the Quick Start Bradford Protein Assay kit (BioRad). An equal amount of protein (*ca.* 200 µg) was incubated with the caspase-3 chromogenic substrate DEVD-*p*NA. The samples were read at 405 nm with a Multiscan Ascent ELISA plate reader, and the absorbance of released *p*NA from AHSV-infected cells was compared to that of uninfected BHK-21 cells. As indicated in Fig. 4, the caspase-3 activity in AHSV-infected BHK-21 cells coincided with the onset and timing of DNA fragmentation (Fig. 3C). Caspase-3 activity was first observed at 12 h post-infection and reached a maximum at 24 h post-infection. Based on these results, it was concluded that AHSV-9 infection of BHK-21 cells induces apoptosis with the activation of the executioner caspase, caspase-3.

Depolarization of the mitochondrial outer membrane is an early, pivotal event in the intrinsic apoptotic signaling pathway (Green and Kroemer, 2004). To evaluate the role of mitochondria in AHSV-induced apoptosis, the mitochondrial membrane potential of AHSV-infected BHK-21 cells was subsequently assessed using DePsipher™ (5,5,6,6-tetrachloro-1,1,3,3-tetraethylbenzimidazolylcarbocyanin iodide) (Trevigen, Inc.). In healthy cells, DePsipher™ has the property of aggregating upon membrane polarization forming a red fluorescent compound with absorption/emission maxima of 585/590 nm. In apoptotic cells the potential is disrupted, the dye cannot access the mitochondrial transmembrane space and remains in its green fluorescent monomeric form with absorption/emission maxima of 510/527 nm. To investigate, control uninfected and AHSV-infected BHK-21 cells (1×10^6 cells/well) were processed at 6-h time intervals post-infection for flow cytometry (BD FACSAria™, BD Biosciences). BHK-21 cells incubated for 24 h with 20 µM of the lypophilic cation FCCP (carbonyl cyanide *p*-[trifluoro-methoxy] phenylhydrazone) served as a positive control for cells

with depolarized mitochondrial membranes (Dispersyn et al., 1999). The results are presented as a green/red fluorescence ratio (geomean FL1/FL2), the increase of which indicates mitochondrial membrane depolarization (Isakovic et al., 2008). Flow cytometric analysis of AHSV-infected BHK-21 cells indicated a progressive loss of mitochondrial membrane potential from 0 to 24 h post-infection, as evidenced by an increase in the green-to-red (FL1/FL2) fluorescence form of the mitochondria-binding dye DePsipher™ (Fig. 5). Indeed, the FL1/FL2 ratio of virus-infected cells at 24 h post-infection was comparable to that obtained for BHK-21 cells incubated with FCCP for 24 h. These results suggest that infection of BHK-21 cells by AHSV-9 resulted in mitochondrial depolarization, and apoptosis induction involves the activation of the intrinsic apoptotic signaling pathway.

Collectively, the results obtained in this study indicated that AHSV induced apoptosis in mammalian cells, but not in insect cells. Although apoptosis in insect cells has been documented (Clarke and Clem, 2003), this finding suggests that the signaling pathway for the induction of apoptosis is not triggered by AHSV infection of insect cells. The results are similar to those reported for other arboviruses that replicate to high titres in both insect vector and vertebrate cells, but show CPE that strongly correlates with the amount of apoptosis only in infected vertebrate cells (Borucki et al., 2002; Courageot et al., 2003; Karpf and Brown, 1998; Li and Stollar, 2004; Mortola et al., 2004). This study more specifically demonstrated that apoptosis is induced in virus-infected mammalian cells via the intrinsic apoptotic pathway, following mitochondrial membrane depolarization that results in subsequent activation of caspase-3. These results are in agreement with those presented for orthoreovirus (Kominsky et al., 2002) and BTV (Nagaleekar et al., 2007), both of which activate the intrinsic apoptosis pathway following loss of mitochondrial membrane potential. However, these results differ from those reported for BTV in which DNA fragmentation is observed at 36 h post-infection and caspase-3 is activated at 24 h post-infection in virus-infected mammalian cells (Mortola et al., 2004; Stewart and Roy, 2010). Interestingly, it has been observed previously that cells infected with AHSV display a much stronger cytopathic effect at early times after infection than cells infected with BTV (Wirblich et al., 2006), suggesting that these two orbiviruses may differ in virulence. Furthermore, the early stage at which mitochondrial depolarization occurs in AHSV-infected BHK-21 cells may indicate that apoptosis is triggered by a virus-induced event early in the infection cycle. In this regard, it is noteworthy that exogenous treatment of mammalian cells with purified recombinant BTV VP2 and VP5 proteins was sufficient to trigger an apoptotic response (Mortola et al., 2004). This would suggest that receptor binding and virus uncoating in the endosome is required for apoptosis. Interestingly, apoptosis induction in reovirus-infected mammalian cells is reported to require viral disassembly in cellular endosomes, but not viral transcription and replication (Connolly and Dermody, 2002). It may therefore be that the process of apoptosis for orbiviruses, such as AHSV and BTV, is very similar to that of orthoreoviruses. Further studies are needed to gain insights into several aspects of AHSV-induced apoptosis, including examining the role of the extrinsic apoptotic pathway in AHSV-induced apoptosis, the identification of viral proteins responsible for inducing apoptosis and the role of AHSV-induced apoptosis in AHSV pathogenesis. Such studies will not only extend knowledge regarding AHSV-host interactions, but may also pave the way to developing new strategies for the prevention and control of AHSV infections.

Acknowledgements

This work was funded by the National Research Foundation.

References

Borucki, M.K., Kempf, B.J., Blitvich, B.J., Blair, C.D., Beaty, B.J., 2002. La Crosse virus: Replication in vertebrate and invertebrate hosts. Microbes Infect. 4, 341-350.

Calisher, C.H., Mertens, P.P.C., 1998. Taxonomy of African horse sickness viruses. Arch. Virol. (Suppl.) 14, 3-11.

Clarke, P., Beckham, J.D., Leser, J.S., Hoyt, C.C., Tyler, K.L., 2009. Fas-mediated apoptotic signaling in the mouse brain following reovirus infection. J. Virol. 83, 6161-6170.

Clarke, P., Tyler, K.L., 2009. Apoptosis in animal models of virus-induced disease. Nature Rev. Microbiol. 7, 144-155.

Clarke, T.E., Clem, R.J., 2003. Insect defenses against virus infection: The role of apoptosis. Int. Rev. Immunol. 22, 401-424.

Coetzer, J.A.W., Erasmus, B.J., 1994. African horsesickness, in: Coetzer, J.A.W., Thomson, G.R., Tustin, R.C. (Eds.), Infectious Diseases of Livestock. Oxford University Press, Cape Town, pp. 460-475.

Connolly, J.L., Dermody, T.S., 2002. Virion disassembly is required for apoptosis induced by reovirus. *J. Virol.* 76, 1632-1641.

Courageot, M.P., Catteau, A., Despres, P., 2003. Mechanisms of Dengue virus-induced cell death. Adv. Virus Res. 60, 157-186.

Dispersyn, G., Nuydens, R., Connors, R., Borgers, M., Geerts, H., 1999. Bcl-2 protects against FCCP-induced apoptosis and mitochondrial membrane potential depolarization in PC12 cells. Biochim. Biophys. Acta 1428, 357-371.

Duprez, L., Wirawan, E., Vanden Berghe, T., Vandenabeele, P., 2009. Major cell death pathways at a glance. Microbes Infect. 11, 1050-1062.

Fischer, U., Jänicke, R.U., Schulze-Osthoff, K., 2003. Many cuts to ruin: A comprehensive update of caspase substrates. Cell Death Differ. 10, 76-100.

Gómez-Villamandos, J.C., Sánchez, C., Carrasco, L., Laviada, M.D., Bautista, M.J., Martínez-Torrecuadrada, J., Sánchez-Vizcaíno, J.M., Sierra, M.A., 1999. Pathogenesis of African horse sickness: Ultrastructural study of the capillaries in experimental infection. J. Comp. Path. 121, 101-116.

Green, D.R., Kroemer, G., 2004. The pathophysiology of mitochondrial cell death. Science 305, 626-629.

Guthrie, A.J., 2007. African horse sickness, in: Sellon, D.C., Long, M. (Eds.), Equine infectious diseases. Suanders Elsevier, Missouri, pp. 164-170.

Isakovic, A., Jankovic, T., Harhaji, L., Kostic-Rajacic, S., Nikolic, Z., Vajs, V., Trajkovic, V., 2008. Antiglioma action of xanthones from Gentiana kockiana: Mechanistic and structure-activity requirements. Bioorg. Med. Chem. 16, 5683-5694.

Karpf, A.R., Brown, D.T. (1998). Comparison of Sindbis virus-induced pathology in mosquito and vertebrate cell cultures. Virology 240, 193-201.

Kerr, J.F., Wyllie, A.H., Currie, A.R., 1972. Apoptosis: A basic biological phenomenon with wide-ranging implications in tissue kinetics. Br. J. Cancer 26, 239-257.

Kominsky, D.J., Bickel, R.J., Tyler, K.L., 2002. Reovirus-induced apoptosis requires both death-receptor- and mitochondrial-mediated caspase-dependent pathways of cell death. Cell Death Differ. 9, 926-933.

Koyama, A.H., Adachi, A., 1997. Induction of apoptosis by herpex simplex virus type 1. J. Gen. Virol. 78, 2909-2912.

Li, M.L., Stollar, V., 2004. Alphaviruses and apoptosis. Int. Rev. Immunol. 23, 7-24.

Martelli, A.M., Zweyer, M., Ochs, R.L., Tazzari, P.L., Tabellini, G., Narducci, P., Bortul, R., 2001. Nuclear apoptotic changes: An overview. J. Cell. Biochem. 82, 634-646.

Mellor, P.S., Hamblin, C., 2004. African horse sickness. Vet. Res. 35, 445-466.

Mirchamsy, H., Hazrati, A., Bahrami, S., Shafyi, A., 1970. Growth and persistent infection of African horse sickness virus in a mosquito cell line. Am. J. Vet. Res. 31, 1755-1761.

Mortola, E., Noad, R., Roy, P., 2004. Bluetongue virus outer capsid proteins are sufficient to trigger apoptosis in mammalian cells. J. Virol. 78, 2875-2883.

Nagaleekar, V.K., Tiwari, A.K., Kataria, R.S., Bais, M.V., Ravindra, P.V., Kumar, S., 2007. Bluetongue virus induces apoptosis in cultured mammalian cells by both caspase-dependent extrinsic and intrinsic apoptotic pahways. Arch. Virol. 152, 1751-1756.

Osawa, Y., Hazrati, A., 1965. Growth of African horse sickness virus in monkey kidney cell cultures. Am. J. Vet. Res. 25, 505-511.

Roulston, A., Marcellus, R.C., Branton, P.E., 1999. Viruses and apoptosis. Annu. Rev. Microbiol. 53, 577-628.

Samuel, M.A., Morrey, J.D., Diamond, M.S., 2007. Caspase-3-dependent cell death of neurons contributes to the pathogenesis of West Nile virus encephalitis. J. Virol. 81, 2614-2623.

Stewart, M.E., Roy, P., 2010. Role of cellular caspases, nuclear factor-kappaβ and interferon regulatory factors in Bluetongue virus infection and cell fate. Virol. J. 7, 362.

Umeshappa, C.S., Singh, K.P., Nanjundappa, R.H., Pandey, A.B., 2010. Apoptosis and immuno-suppression in sheep infected with bluetongue virus serotype-23. Vet. Microbiol. 144, 310-318.

Wilson, A., Mellor, P.S., Szmaragd, C., Mertens, P.P.C., 2009. Adaptive strategies of African horse sickness virus to facilitate vector transmission. Vet. Res. 40, 16.

Wirblich, C., Bhattacharya, B., Roy, P., 2006. Nonstructural protein 3 of bluetongue virus assists virus release by recruiting ESCRT-I protein Tsg101. J. Virol. 80, 460-473.

Wyllie, A.H., 1980. Glucocorticoid-induced thymocyte apoptosis is associated with endogenous endonuclease activation. Nature 284, 555-556.

Wyllie, A.H., Beattie, G.J., Hargreaves, A.D., 1981. Chromatin changes in apoptosis. Histochem. J. 13, 681-692.

Figure captions

Fig. 1 AHSV-9 induces apoptosis in mammalian cells. (A) Immunoblot analysis of cell lysates from mock-infected (P) and AHSV-infected BHK-21 cells over a time course of 72 h using an AHSV-9 antiserum. The sizes of the molecular weight marker (M; Fermentas) are indicated to the left of the figure. (B) Micrographs of

mock-infected and AHSV-infected BHK-21 cells at 72 h post-infection. In contrast to mock-infected cells, AHSV-infected cells show clear signs of shrinkage, rounding and detachment. Bar = 50 µm. (C) Transmission electron micrographs of mock-infected and AHSV-infected BHK-21 cells taken at 72 h post-infection. Representative fields are shown. In contrast to mock-infected BHK-21 cells, AHSV-infected cells show morphological hallmarks of apoptosis, as indicated by the arrows. These included condensation of chromatin, the formation of apoptotic bodies and plasma membrane blebbing. Bar = 1 µm.

Fig. 2 AHSV-9 does not induce apoptosis in insect cells. (A) Immunoblot analysis of cell lysates from mock-infected (P) and AHSV-infected KC cells over a time course of 7 days using an AHSV-9 antiserum. The sizes of the molecular weight marker (M; Fermentas) are indicated to the left of the figure. (B) Micrographs of mock-infected and AHSV-infected KC cells at 7 days post-infection, indicating a lack of CPE. Bar = 40 µm. (C) Transmission electron micrographs of mock-infected and AHSV-infected KC cells taken at 7 days post-infection showing no detectable morphological hallmarks of apoptosis. Representative fields are shown. Bar = 1 µm.

Fig. 3 DNA fragmentation analysis of BHK-21 and KC cells infected with AHSV-9. (A) Agarose gel electrophoretic pattern of chromosomal DNA extracted from mock-infected (P) and AHSV-infected BHK-21 cells at different times post-infection (12 - 72 h). Apoptotic U937 cells served as a positive control (+). (B) Agarose gel electrophoretic pattern of chromosomal DNA extracted from mock-infected (P) and AHSV-infected KC cells over a time course of 7 days. The sizes of the molecular weight marker, GeneRuler™ 1 kb DNA ladder (Fermentas), are indicated to the left of the figure. (C) Enrichment of nucleosomes in the cytoplasm of BHK-21 cells infected with AHSV-9. Cytoplasmic extracts were prepared from AHSV-infected BHK-21 cells at different time intervals post-infection, transferred into a streptavidin-coated microtitre plate and incubated with a mixture of anti-histone-biotin and anti-DNA-peroxidase antibodies. The nucleosomes were detected by measuring peroxidase activity, and the nucleosome enrichment factor was subsequently calculated. The data are means ± SD of two independent experiments.

Fig. 4 Activation of caspase-3 associated with AHSV-induced apoptosis in BHK-21 cells. Cytoplasmic extracts, each containing 200 µg total protein, were prepared from uninfected and AHSV-infected BHK-21 cells at different times post-infection. Following incubation with the caspase-3 synthetic substrate DEVD-*p*NA, the liberated *p*NA was quantified at 405 nm in an ELISA plate reader. The data is presented as an increase in caspase-3 activity. Data are expressed as mean ± SD of three independent experiments.

Fig. 5 Mitochondrial membrane depolarization in BHK-21 cells infected with AHSV-9. AHSV-infected BHK-21 cells were treated with DePsipher™ at the indicated times post-infection, and analyzed by flow cytometry. BHK-21 cells treated with FCCP were included as a positive control in the analysis. The green Desipher™ monomers were detected using the fluorescein channel (FITC-A; FL1), and the red Desipher™ aggregates were detected using the propidium iodide channel (PE-A; FL2). An increase in the ratio of green (FL1)/red (FL2) fluorescence is indicative of mitochondrial membrane depolarization. Results are mean values ± SD of two independent experiments.

Fig. 1

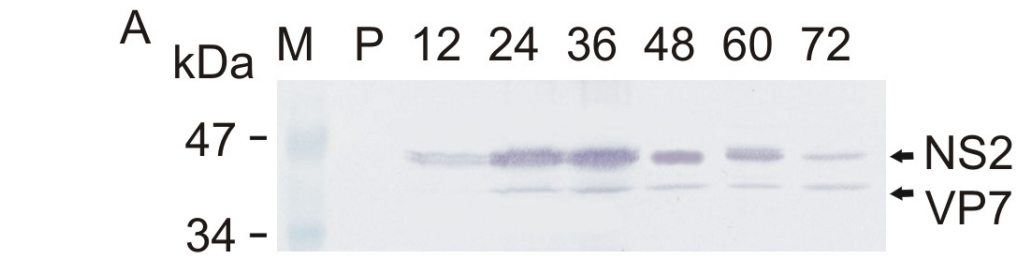

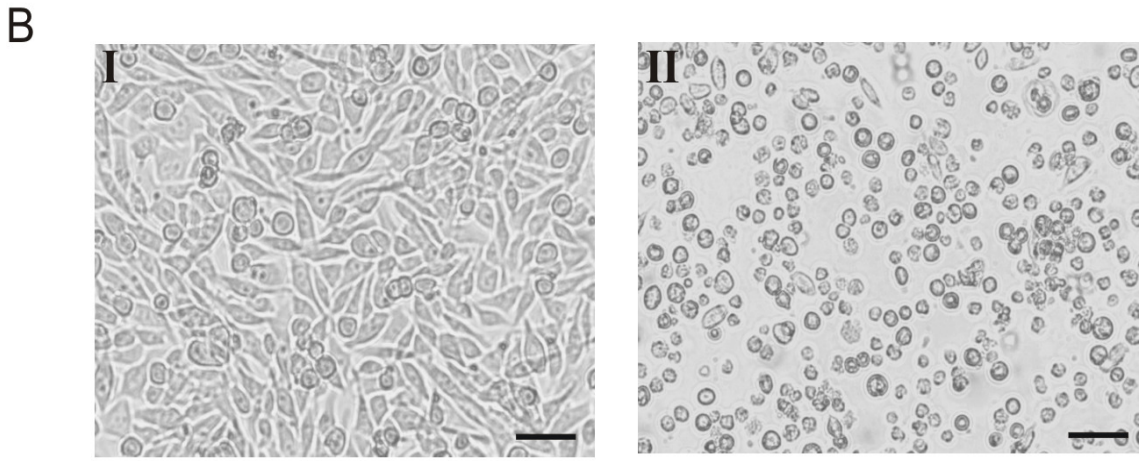

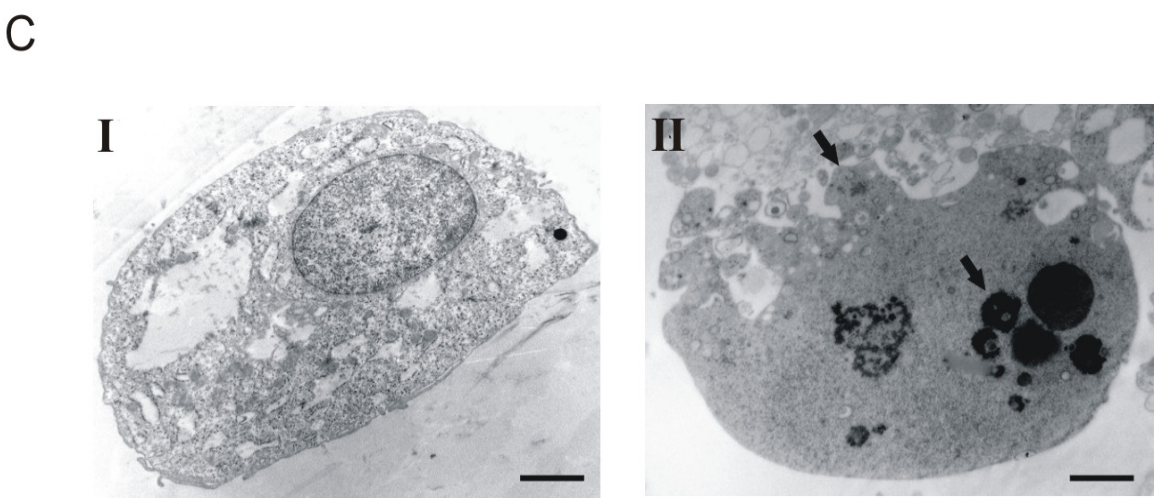

Fig. 2

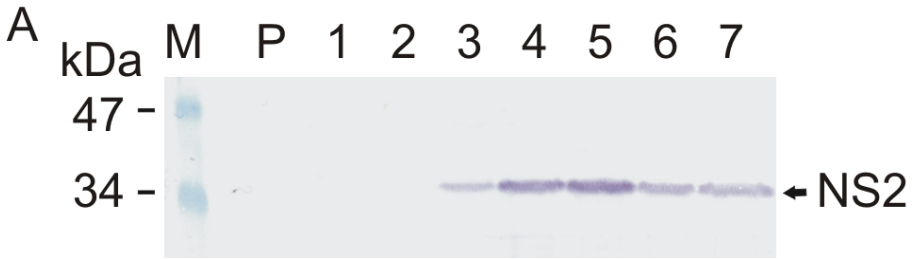

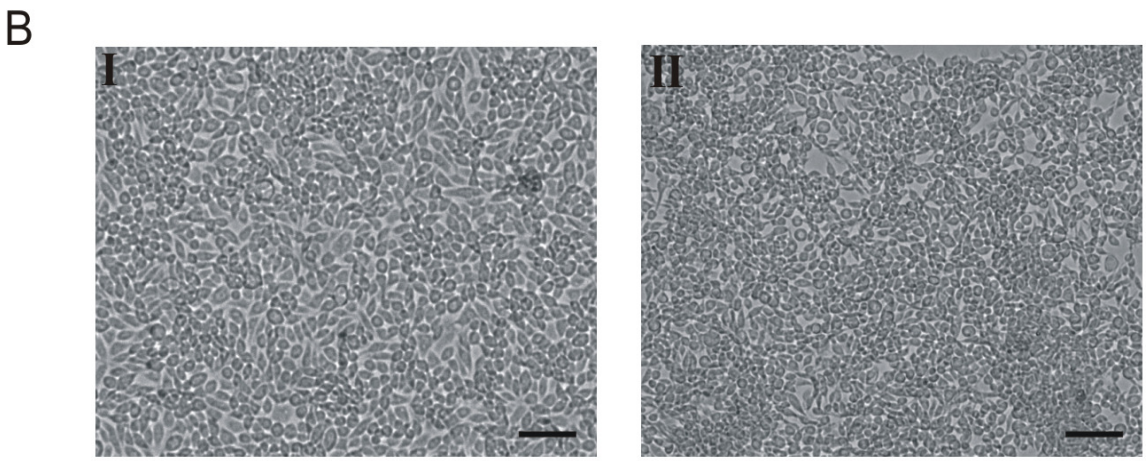

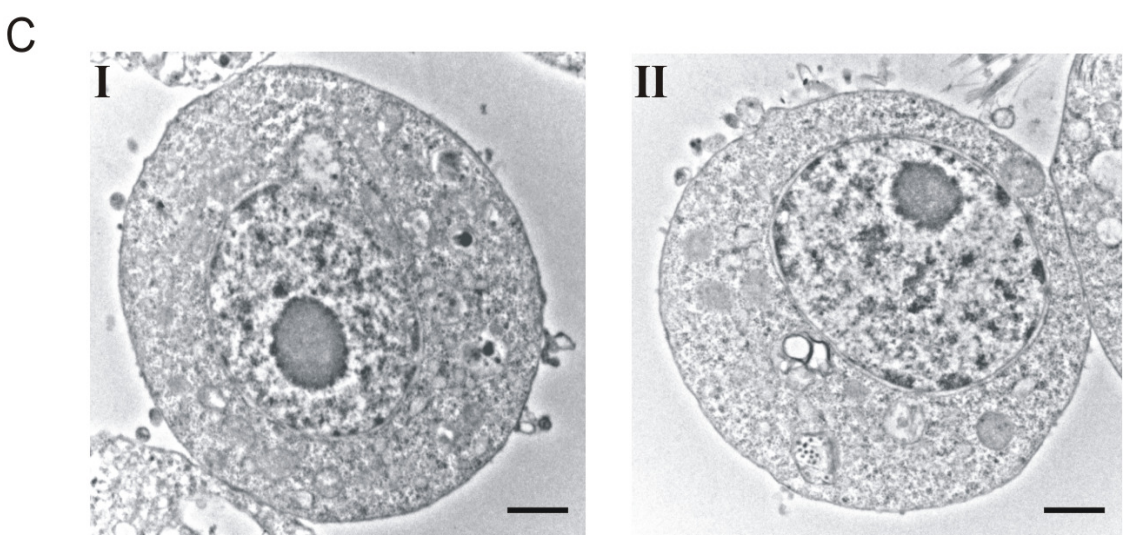

Fig. 3A

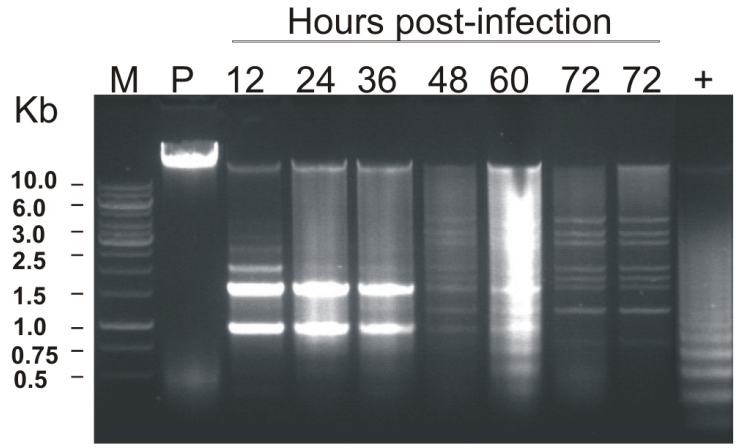

Fig. 3B

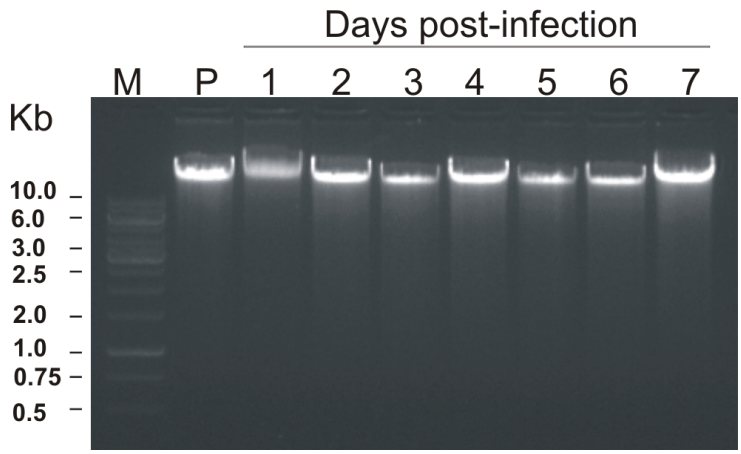

Fig. 3C

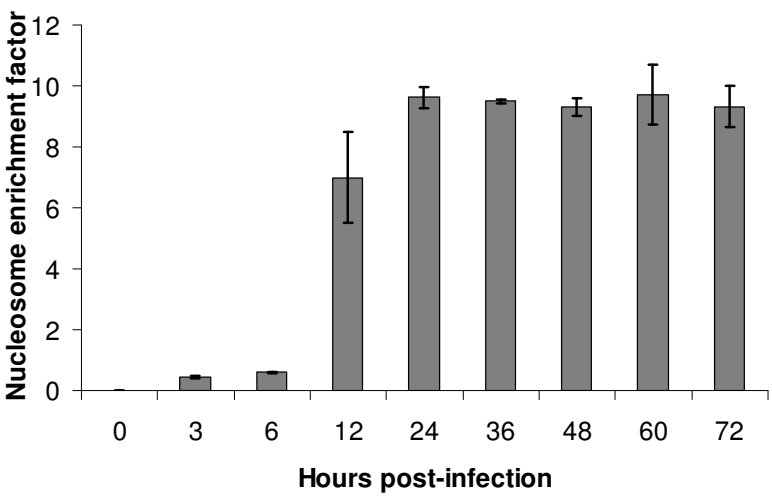

Fig. 4

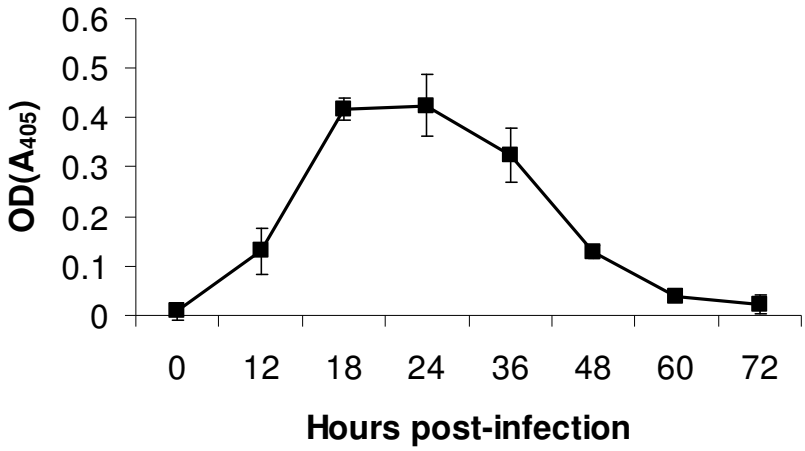
0.6
0.5
0.4
0.3
0.2
0.1
0
OD(A405)
0
12
18
24
36
48
60
72
Hours post-infection

Fig. 5

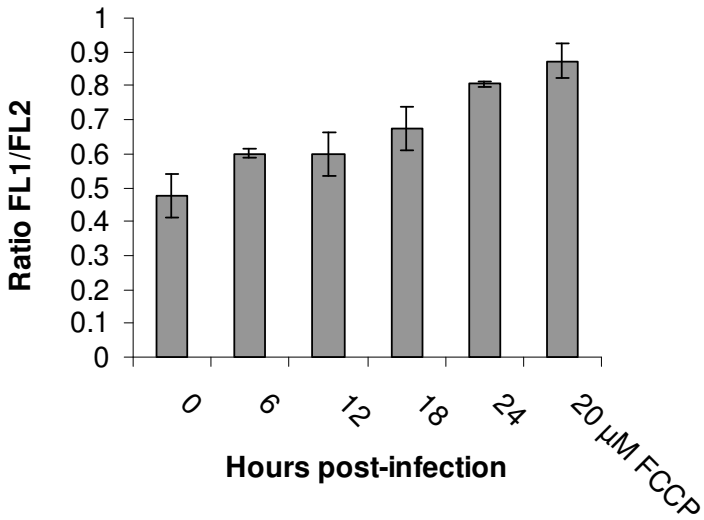
Ratio FL1/FL2
1
0.9
0.8
0.7
0.6
0.5
0.4
0.3
0.2
0.1
0
0
6
12
18
24
20 µM FCCP
Hours post-infection

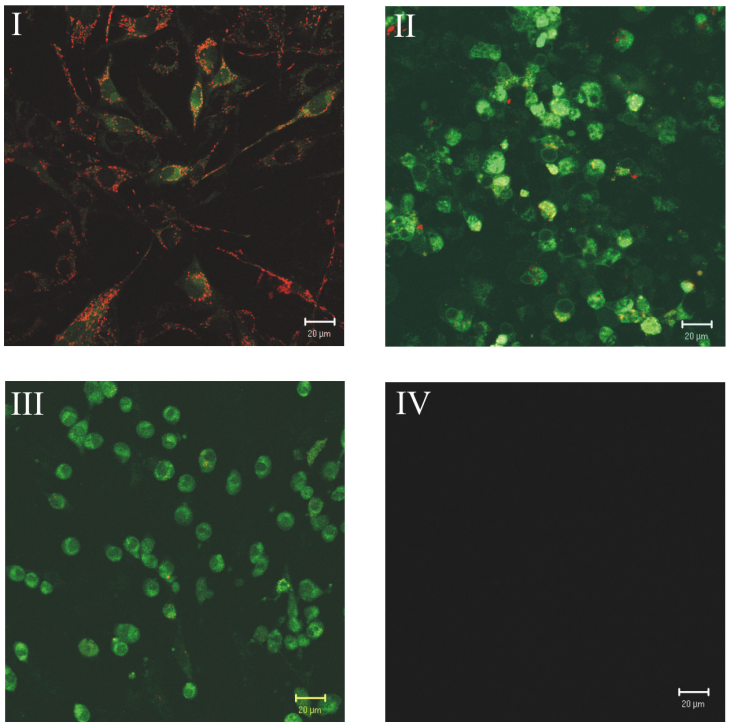

Confocal scanning laser microscopy of AHSV-infected BHK-21 cells stained with DePsipher™. Uninfected BHK-21 cells (I), AHSV-infected BHK-21 (II) and BHK-21 cells treated with FCCP (III) were examined at 24 h post-infection with a Zeiss LSM S10 META confocal microscope fitted with bypass filters for fluorescein (505-550 nm) and rhodamine (560-615 nm). Representative fields are shown. No fluorescence was observed in uninfected BHK-21 cells without the DePsipher™ reagent (IV). Bar = 20 µm.